

Robustness of the nodal d -wave spectrum to strongly fluctuating competing order

W. A. Atkinson^{1,*}, J. David Bazak¹, and B. M. Andersen²

¹*Department of Physics and Astronomy, Trent University, Peterborough Ontario, Canada, K9J 7B8*

²*Niels Bohr Institute, University of Copenhagen, DK-2100 Copenhagen, Denmark*

(Dated: November 8, 2018)

We resolve an existing controversy between, on the one hand, convincing evidence for the existence of competing order in underdoped cuprates, and, on the other hand, spectroscopic data consistent with a seemingly homogeneous d -wave superconductor in the very same compounds. Specifically, we show how short-range fluctuations of the competing order essentially restore the nodal d -wave spectrum from the qualitatively distinct folded dispersion resulting from homogeneous coexisting phases. The signatures of the fluctuating competing order can be found mainly in a splitting of the antinodal quasi-particles and, depending of the strength of the competing order, also in small induced nodal gaps as found in recent experiments on underdoped $\text{La}_{2-x}\text{Sr}_x\text{CuO}_4$.

Many recent experiments point to the prominence of competing phases in underdoped cuprate superconductors, and challenge existing theories for the pseudogap phase.[1–12] Evidence has been found for stripe phases in the La_2CuO_4 [13, 14] and $\text{YBa}_2\text{Cu}_3\text{O}_{6+x}$ families,[11, 15–17] checkerboard and nematic phases in the Bi-based cuprates,[18–20] loop-current order in $\text{YBa}_2\text{Cu}_3\text{O}_{6+x}$,[21] and spin glass phases in most of the highly underdoped cuprates.[22–24] All of these phases are expected to have clear spectroscopic signatures which, in many cases, involve a Fermi surface reconstruction; puzzlingly, however, angle resolved photoemission spectroscopy (ARPES), which has become a powerful probe of the electronic structure of the high temperature superconductors, finds no clear evidence of any reconstruction,[25–28] even for materials like $\text{La}_{2-x}\text{Sr}_x\text{CuO}_4$ (LSCO) near $x = 1/8$ where signatures of reconstruction due to stripes are expected to be maximal.[29, 30] A few recent studies report antinodal (AN) particle-hole symmetry breaking in the pseudogap phase of $\text{Pb}_{0.55}\text{Bi}_{1.55}\text{Sr}_{1.6}\text{La}_{0.4}\text{CuO}_{6+\delta}$ (Bi2201),[10, 31] thus confirming the presence of competing order, but the underlying low-temperature dispersion of the electronic quasi-particles in the nodal region remains remarkably similar to that of a well-known d -wave superconductor. This is still true even in the insulating spin-glass regime at doping levels so low that superconductivity is not yet present.[27] In many cases, the competing order appears to be fluctuating rather than static,[16, 22] and in this paper we demonstrate that many aspects of the ARPES spectrum, such as the robustness of the nodal d -wave spectrum to strong competing order, can be understood if this fact is accounted for.

Motivated by the widespread observation of short-range slow antiferromagnetic (AF) fluctuations in underdoped cuprates, we focus on the competition between AF and d -wave superconducting (dSC) order, but we expect our main results may apply also to other candidates for the competing order. Specifically, we have performed Monte Carlo (MC) simulations of a two-dimensional dSC in which thermal fluctuations of both the AF and dSC

order parameters are included. Our main finding is that highly inhomogeneous phases, which are widely reported experimentally, qualitatively alter the low-energy quasi-particle dispersion from the homogeneous or weakly disordered situation. We find that: (1) unless the competing order is very strong, the spectrum is indistinguishable from that of the pure dSC, (2) even for strong competing order the nodal electronic spectrum is very similar to that of the pure superconductor, and shows no sign of Fermi surface reconstruction expected from AF order, and (3) when the competing order is strong, the AN gap has a distinct energy scale from the nodal region. These results bridge the seemingly contradictory findings of simple momentum-space behavior reported by ARPES versus complex inhomogeneous real-space behavior reported by local probes.

Our main results are illustrated by Fig. 1, where spectra are shown for a pure dSC and for a dSC with strong competing magnetism (dSC+AF). The top panels (a-d) show snapshots, taken from the MC simulation, of the dSC amplitude $\Delta_d(\mathbf{r}_i)$ (b,d) and of the local AF moment $m_Q(\mathbf{r}_i)$ (a,c). The bottom panels (f,g) show the spectral function $A(\mathbf{k}, \omega)$ at \mathbf{k} -points taken along the nodal and AN lines shown in 1(e). The spectral function shown in Fig. 1(f) [Fig. 1(g)] arises from sampling of configurations similar to (a,b) [(c,d)]. For comparison, in Fig. 1(h) we also show spectra for the simplified case when dSC and AF order coexist homogeneously. In this case, we use the root-mean-square values of the AF and dSC order parameters from 1(g).

The similarity between the nodal spectra for the pure dSC [Fig. 1(f)] and dSC+AF [Fig. 1(g)] is remarkable, especially in comparison to the uniformly coexisting case [Fig. 1(h)]. In the uniform case, the nodal cut exhibits the well-known band back-folding that results in the formation of closed Fermi surface pockets around the AF Brillouin zone boundary. The back-folding is due to the large AF-induced band gap that appears above the Fermi energy. It is striking that the band gap is completely absent in 1(g); instead, the dispersion is almost indistinguishable from that of the pure dSC despite the presence

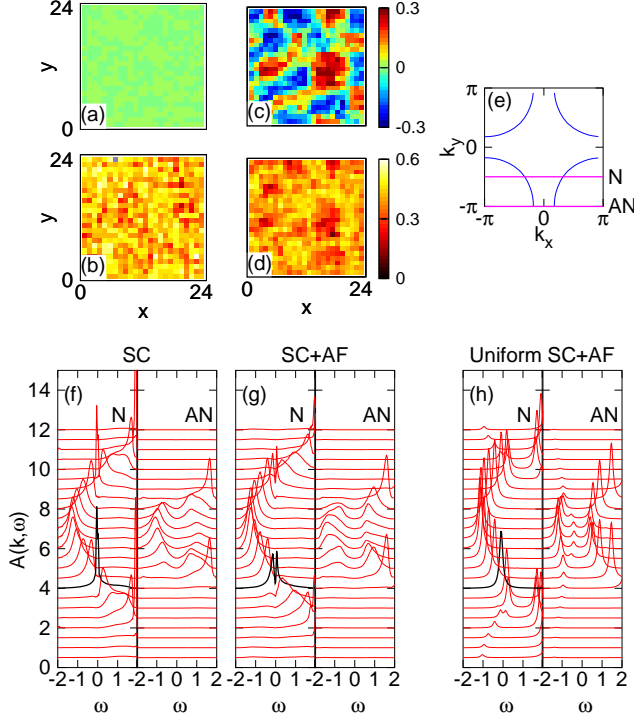


FIG. 1: (Color online) (a-d) Snapshots of MC simulations for (a,b) a pure dSC and (c,d) a dSC with competing AF order at reduced temperature $\tau = T/T_c = 0.3$. (a,c) The local AF moment $m_Q(\mathbf{r}_i)$ and (b,d) dSC order parameter are shown for the final step in the MC simulation. (f-h) The averaged spectral function is shown along nodal (N) and antinodal (AN) cuts illustrated in (e). The spectra are for (f) dSC only, (g) dSC+AF, and (h) a homogeneously coexisting dSC and AF. Linewidths are due to thermal fluctuations, except in (h) where they are artificial. In all cases, the filling is $n \approx 0.88$. Parameters are $V = -1.0$ and (a,b) $U = 0$, for which $T_c = 0.20$ and (c,d) $U = 3.5$, for which $T_c = 0.06$. The Fermi energy is $\varepsilon_F = 0$ throughout. In (h) we set $\Delta_d = 0.35$ and $Um_Q = 3.5 \times 0.2$ based on average values in (g).

of sizable magnetic moments on nearly all sites evident from Fig. 1(c). The only signature of the competing magnetism is the narrow nodal gap at the Fermi energy in 1(g) similar to what has been recently found in ARPES studies of underdoped LSCO.[32] We stress that in our model, the nodal gap appears only for large values of U , close to the superconductor-insulator transition; at smaller values of U , the nodal dispersion remains indistinguishable from the pure dSC case.

In contrast to the nodal spectrum, the AN spectrum in (g) resembles that of the uniform dSC+AF case in (h): the single quasiparticle peak at $\omega < \varepsilon_F$ in (f) is split into a pair of peaks in (g) and (h), one of which is upward-dispersing and the other of which is downward-dispersing. While the splitting is obvious in (h), the peaks are not easily resolved in (g) because the line shapes are thermally broadened, and the lower intensity peak appears as a shoulder.

The results shown in Fig. 1(g) are qualitatively similar to what has been reported at low T for ARPES experiments on Bi2201,[10, 31] namely, there is a band splitting at the antinode but no sign of Fermi surface reconstruction near the node. We emphasize that, while it is possible to model the AN spectrum with a uniform “finite- q ” spin or charge density wave, as in Ref. 31, it is much more difficult to model the spectrum along the entire Fermi surface that way. Indeed, Norman *et al.*[33] have argued against finite- q models of the pseudogap for this reason. Figure 1(g) shows that fluctuations qualitatively alter the spectrum in a way that is consistent with experiments.

Figure 1 is based on MC simulations on an $L \times L$ lattice of electrons coupled to two thermally fluctuating classical fields. The real field h_i couples to the local magnetization at site i while the complex field d_{ij} couples to Cooper pairs along bonds connecting nearest-neighbor sites i and j . Purely superconducting models (with $h_i = 0$) have been widely used to study phase fluctuations,[34–38] but relatively little work has focussed on the more complicated problem of competing order.[39–41] The partition function is

$$Z = \int D[hdd^*] \exp[-\beta\Omega(h, d)], \quad (1)$$

where $\Omega(h, d) = -T \ln [\text{Tr} \exp(-\beta\hat{H})]$, $\text{Tr} \dots$ is a trace over electronic degrees of freedom, $\int D[hdd^*] \dots$ is a $5L^2$ -dimensional integral over the fields, and

$$\hat{H} = \sum_{ij\sigma} t_{ij} c_{i\sigma}^\dagger c_{j\sigma} - \sum_{i\sigma} \sigma h_i \hat{n}_{i\sigma} + \sum_i \frac{h_i^2}{U} + \sum_{ij} \left[d_{ij} c_{i\uparrow}^\dagger c_{j\downarrow}^\dagger + d_{ij}^* c_{j\downarrow} c_{i\uparrow} - \frac{|d_{ij}|^2}{V} \right]. \quad (2)$$

In Eq. (2), t_{ij} are the hopping matrix elements between nearest ($t_{ij} = -t = -1$; t is the unit of energy throughout this work) and next-nearest ($t_{ij} = t' = 0.4$) neighbors. To reduce the number of integration variables, we impose the singlet constraint $d_{ij} = d_{ji}$. U and V control the size of the AF and SC fluctuations respectively; at $T = 0$, the saddle point approximation is exact and gives $h_i = Um(\mathbf{r}_i)$ where $m(\mathbf{r}_i) = \langle \hat{n}_{i\uparrow} - \hat{n}_{i\downarrow} \rangle / 2$ and $d_{ij} = V \langle c_{j\downarrow} c_{i\uparrow} \rangle$. Throughout this work, we fix the pairing interaction to be $V = -1.0$ and vary the Coulomb repulsion U . The dSC order parameter is $\Delta_d(\mathbf{r}_i) = \sum_j (-1)^{y_i - y_j} \langle c_{j\downarrow} c_{i\uparrow} \rangle$, where j is summed over nearest neighbors of i , and the AF moment is $m_Q(\mathbf{r}_i) = (-1)^{x_i + y_i} m(\mathbf{r}_i)$. The dSC transition occurs at the temperature T_c where the pair correlation $\Delta_d(\mathbf{r}_i) \Delta_d^*(\mathbf{r}_i + \mathbf{R}) = 0$, with $\mathbf{R} = \frac{1}{2}(L, L)$.

We use a Metropolis algorithm to evaluate the integral in Eq. (1). To reduce noise, all spectra are averaged over 10-20 separate MC simulations; a typical simulation consists of 2×10^4 sweeps, where one sweep has L^2 steps, in which each field is updated. The MC calculations are

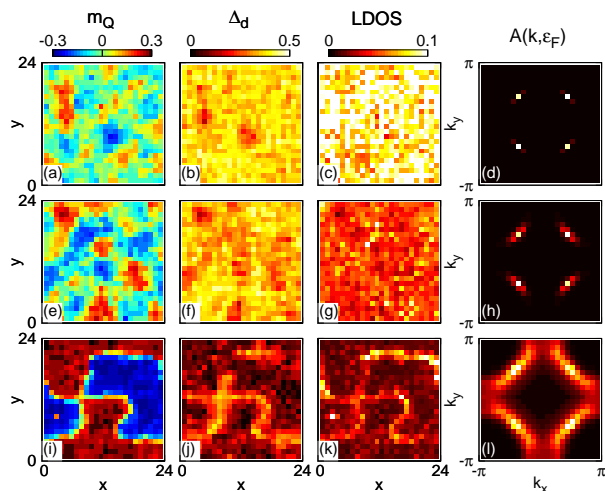


FIG. 2: (Color online) Results of MC simulations at $T = 0.02$ for three different U values. Results are for (a-d) $U = 3.3$, (e-h) $U = 3.5$, and (i-l) $U = 3.8$. First and second columns contain MC snapshots of $m_Q(\mathbf{r}_i)$ and $\Delta_d(\mathbf{r}_i)$ respectively; the third column contains the LDOS corresponding to the configuration in the first two columns. The final column shows the MC-averaged spectral function $A(\mathbf{k}, \varepsilon_F)$.

computationally demanding because \hat{H} must be diagonalized at each step; in similar calculations[39] systems were limited to $L \leq 12$ sites (see, however, [37] for an alternative approach). Here, we use first order perturbation theory to estimate updates to $\Omega(h, d)$ at each MC step, with a full diagonalization of \hat{H} at the beginning of each MC sweep. We have checked that this does not change the MC-generated distribution of h_i and d_{ij} values, and can study systems up to $L = 32$ by this method.

Typical m_Q and Δ_d configurations sampled by the MC simulations shown in Fig. 2 illustrate how the model evolves with increasing U . For $U = 3.3$ [Fig. 2(a)], there are large regions where $m_Q(\mathbf{r}_i)$ is small, and small pockets of short-lived AF order. The dSC order parameter also fluctuates [Fig. 2(b)], and there is a clear spatial anticorrelation between $\Delta_d(\mathbf{r}_i)$ and $m_Q(\mathbf{r}_i)$. In 2(c), we have plotted the local density of states (LDOS) at the Fermi energy, calculated for the particular configuration of $m_Q(\mathbf{r}_i)$ and $\Delta_d(\mathbf{r}_i)$ shown in 2(a) and 2(b). The LDOS is reduced inside the AF pockets, and is largest in regions where the AF moments are small. Finally, in 2(d), we show the MC-averaged spectral function at ε_F . It is apparent that the nodal quasiparticles are largely unaffected by the fluctuations, so that the low energy spectral weight is concentrated at the four nodal points.

The AF fluctuations are larger when $U = 3.5$ [Fig. 2(e)], and Δ_d is suppressed in a significant fraction of the sample, although the maximum value of Δ_d in 2(f) is about the same as in 2(b). The tendency for the low energy LDOS, shown in 2(g), to be concentrated along AF domain walls is more pronounced than in 2(c), and

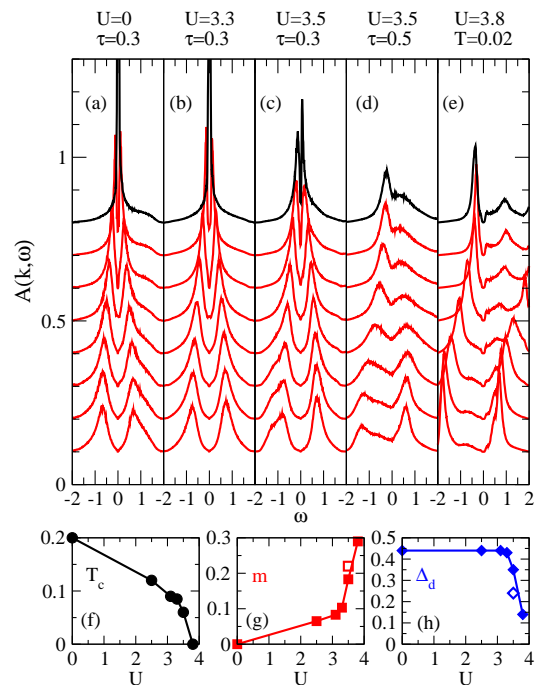


FIG. 3: (Color online) Spectral function $A(\mathbf{k}, \omega)$ along the Fermi surface. Curves (offset for clarity) are taken at \mathbf{k} -points between the nodal point (top curve) to the AN point (bottom curve). Panels (a)-(e) correspond to different U or reduced temperature $\tau = T/T_c$, and are arranged in order of increasing average magnetic moment. T_c values are shown in (f); root-mean-square averaged (g) m and (h) Δ_d is shown at $\tau = 0.3$ (solid symbols) and $\tau = 0.5$ for $U = 3.5$ (open symbols).

becomes even more pronounced when $U = 3.8$, Fig. 2(k), where there is now phase separation. In this case, mobile holes lie almost entirely at the boundaries between AF domains; there is some residual pairing of the holes [Fig. 2(j)], but there is no long-range phase coherence and the system is non-superconducting.

The spectral function at ε_F for $U = 3.8$ shown in Fig. 2(l) reveals very little of the complex real-space structure that emerges as U increases. Indeed, the main change is that the nodal points in Fig. 2(d) evolve into “Fermi arcs” with increasing U . That AF fluctuations contribute to arc formation was suggested previously in Ref. 40; here we add the observation that this persists even into the nonsuperconducting state. Indeed, it is remarkable that one recovers the underlying “bare” Fermi surface purely from states along the spaghetti-like domain walls. This situation is reminiscent of the low-energy spectral features studied in the case of disordered stripes,[42–44] which, however, assumed perfect order along one spatial direction leading to a characteristic Fermi surface reconstruction.

Next, we show in Fig. 3 the progressive evolution of $A(\mathbf{k}, \omega)$ as the magnetic fluctuations are increased. The spectra are taken at momenta along the Fermi surface between the nodal and the AN points. To obtain good mo-

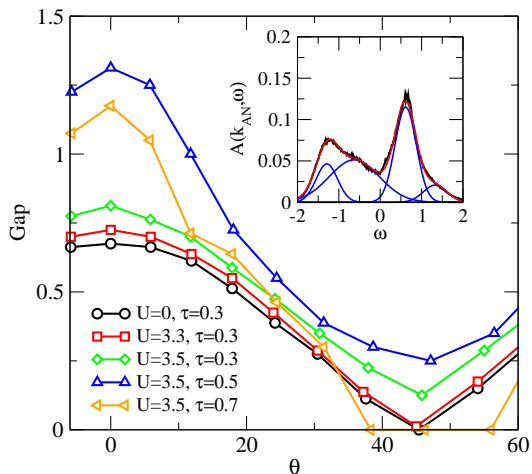


FIG. 4: (Color online) Spectral gap along the Fermi surface for different U and reduced temperature τ . The angle θ is measured along the Fermi surface, with $\theta = 0$ corresponding to the antinode and $\theta = 45^\circ$ to the node. *Inset*: Decomposition of the antinodal spectrum into gaussians for $U = 3.5$, $\tau = 0.5$.

mentum resolution, we calculated the spectrum at points that are interpolated between the L^2 \mathbf{k} -points of the original simulation as follows: after the MC simulations were completed, we recalculated the spectrum with a complex boundary condition using the previously-generated sequence of h_i and d_{ij} values. The complex phases were tuned to shift the \mathbf{k} -values to the Fermi surface (a different phase is required for each \mathbf{k} -point). In panels (a-c) $A(\mathbf{k}, \omega)$ is shown for increasing U at the same reduced temperature $\tau \equiv T/T_c = 0.3$, and the root-mean-square values of Δ_d and m at this τ are plotted in 3(g) and 3(h), respectively. In 3(d), $\tau = 0.5$, which increases m and lowers Δ_d , as shown by the open symbols in 3(g) and 3(h). Finally, in 3(e), spectra are shown for the phase-separated system at low T .

In agreement with the main conclusions from Fig. 1, Fig. 3(b) is essentially indistinguishable from Fig. 3(a), even though T_c is reduced by a factor of two by AF fluctuations [Fig. 3(f)]. Small differences from the d -wave spectrum only emerge in 3(c), by which point T_c is one third of its value in 3(a). In 3(c), a small gap appears at the node and the AN peak below ε_F splits into two. These features are more pronounced in 3(d), where the AF fluctuations are larger. Finally, in 3(e), there is a reorganization of the electronic structure into lower and upper magnetic bands. It is the small residual spectral weight near ε_F , coming from the AF domain walls, which generates the Fermi surface in Fig. 2(l).

As mentioned above, a recent comprehensive ARPES study of LSCO has discovered that the excitation spectrum is gapped along the entire underlying Fermi surface, and hence displays a nodal gap, in the highly underdoped regime.[32] At doping levels where the nodal

gap is observed, a spin glass is known to coexist with superconductivity,[22] and in Fig. 4 we show that AF fluctuations can indeed generate a nodal gap.

Figure 4 shows how the gap along the Fermi surface depends on both the magnitude and the correlation length of the AF fluctuations. To be consistent with experiments, we define the gap at a point \mathbf{k} on the Fermi surface as the position of the highest-lying peak in $A(\mathbf{k}, \omega)$ for $\omega < \varepsilon_F$. When $U \leq 3.3$, the gap along the Fermi surface has a dSC-like structure, and is characterized by a single energy scale. When AF correlations are stronger (see e.g. the $U = 3.5$, $\tau = 0.3$ curve) the AN gap remains set by the dSC scale, and a second energy scale emerges in the form of a small gap at the node, similar to what was found by Razzoli *et al.*[32] In Fig. 4 the nodal gap grows with the AF magnitude, but vanishes at high temperature when the AF correlation length is short and line broadening wipes it out. A third energy scale emerges at the AN when AF correlations are strong ($U = 3.5$ and $\tau \geq 0.5$). In this case a large gap, with an energy scale distinct from that near the node, develops. Similar crossovers between a superconducting nodal gap and nonsuperconducting AN gap have been widely seen in ARPES experiments on many underdoped cuprates;[1, 3, 6, 7, 10, 12] that this is not reported in LSCO suggests that AF correlations are not strong enough for a clear AN feature to develop.

We have found that, even when they cannot be resolved by eye, two energy scales are always present in the AN spectrum when U is large (Fig. 4 inset). The inner peak has a d -wave \mathbf{k} -space structure, while the outer peak is tied to the AF fluctuations, although it is not simply related to the magnetic energy scale $Um \sim 0.7$. To confirm AF correlations as the source of the nodal gap in LSCO, our calculations suggest that one should look for a second energy scale, particularly in the AN spectrum. This would distinguish spin glass physics from models (such as $d + id$ pairing[32]) in which the gaps are added in quadrature.

In conclusion, we have shown that the overall spectrum measured by ARPES experiments is consistent with simple models of competing order if one accounts for the highly inhomogeneous nature of the competing phases. Such models explain the origin of the robust electronic states in momentum space arising from complex real-space environments with substantial amplitudes of the fluctuating competing order.

W.A.A. and J.D.B. acknowledge support by the Natural Sciences and Engineering Research Council (NSERC) of Canada. B.M.A. acknowledges support from The Danish Council for Independent Research | Natural Sciences. This work was made possible by the facilities of the Shared Hierarchical Academic Research Computing Network (SHARCNET:www.sharcnet.ca) and Compute/Calcul Canada.

-
- * Electronic address: billatkinson@trentu.ca
- [1] K. Tanaka, W. S. Lee, D. H. Lu, A. Fujimori, T. Fujii, Risdiana, I. Terasaki, D. J. Scalapino, T. P. Devereaux, Z. Hussain, et al., *Science* **314**, 1910 (2006).
 - [2] M. Le Tacon, A. Sacuto, A. Georges, G. Kotliar, Y. Gallais, D. Colson, and A. Forget, *Nature Physics* **2**, 537 (2006).
 - [3] W. S. Lee, I. M. Vishik, K. Tanaka, D. H. Lu, T. Sasagawa, N. Nagaosa, T. P. Devereaux, Z. Hussain, and Z. X. Shen, *Nature* **450**, 81 (2007).
 - [4] N. Doiron-Leyraud, C. Proust, D. LeBoeuf, J. Levallois, J.-B. Bonnemaïson, R. Liang, D. A. Bonn, W. N. Hardy, and L. Taillefer, *Nature* **447**, 565 (2007).
 - [5] S. Hufner, M. A. Hossain, A. Damascelli, and G. A. Sawatzky, *Rep. Prog. Phys.* **71**, 062501 (2008).
 - [6] J.-H. Ma, Z.-H. Pan, F. C. Niestemski, M. Neupane, Y.-M. Xu, P. Richard, K. Nakayama, T. Sato, T. Takahashi, H.-Q. Luo, et al., *Phys. Rev. Lett.* **101**, 207002 (2008).
 - [7] T. Kondo, R. Khasanov, T. Takeuchi, J. Schmalian, and A. Kaminski, *Nature* **457**, 296 (2009).
 - [8] T. Kondo, Y. Hamaya, A. D. Palczewski, T. Takeuchi, J. S. Wen, Z. J. Xu, G. Gu, J. Schmalian, and A. Kaminski, *Nature Physics* **7**, 21 (2010).
 - [9] R. Daou, J. Chang, D. LeBoeuf, O. Cyr-Choinière, F. Laliberté, N. Doiron-Leyraud, B. J. Ramshaw, R. Liang, D. A. Bonn, W. N. Hardy, et al., *Nature* **463**, 519 (2010).
 - [10] R.-H. He, M. Hashimoto, H. Karapetyan, J. D. Koralek, J. P. Hinton, J. P. Testaud, V. Nathan, Y. Yoshida, H. Yao, K. Tanaka, et al., *Science* **331**, 1579 (2011).
 - [11] T. Wu, H. Mayaffre, S. Krämer, M. Horvatic, C. Berthier, W. N. Hardy, R. Liang, D. A. Bonn, and M.-H. Julien, *Nature* **477**, 191 (2011).
 - [12] S.-I. Ideta, T. Yoshida, A. Fujimori, H. Anzai, T. Fujita, A. Ino, M. Arita, H. Namatame, M. Taniguchi, Z.-X. Shen, et al., *Phys. Rev. B* **85**, 104515 (2012).
 - [13] S. A. Kivelson, I. P. Bindloss, E. Fradkin, V. Oganesyan, J. M. Tranquada, A. Kapitulnik, and C. Howald, *Rev. Mod. Phys.* **75**, 1201 (2003).
 - [14] J. M. Tranquada, *Handbook of High-Temperature Superconductivity Theory and Experiment*, edited by J. R. Schrieffer (2007).
 - [15] V. Hinkov, D. Haug, B. Fauqué, P. Bourges, Y. Sidis, A. Ivanov, C. Bernhard, C. T. Lin, and B. Keimer, *Science* **319**, 597 (2008).
 - [16] D. Haug, V. Hinkov, Y. Sidis, P. Bourges, N. B. Christensen, A. Ivanov, T. Keller, C. T. Lin, and B. Keimer, *New J. of Phys.* **12**, 105006 (2010).
 - [17] G. Ghiringhelli and M. Le Tacon, preprint (2012).
 - [18] C. Howald, H. Eisaki, N. Kaneko, M. Greven, and A. Kapitulnik, *Phys. Rev. B* **67**, 014533 (2003).
 - [19] M. Vershinin, S. Misra, S. Ono, Y. Abe, Y. Ando, and A. Yazdani, *Science* **303**, 1995 (2004).
 - [20] Y. Kohsaka, C. Taylor, K. Fujita, A. Schmidt, C. Lupien, T. Hanaguri, M. Azuma, M. Takano, H. Eisaki, H. Takagi, et al., *Science* **315**, 1380 (2007).
 - [21] B. Fauqué, Y. Sidis, V. Hinkov, S. Pailhès, C. T. Lin, X. Chaud, and P. Bourges, *Phys. Rev. Lett.* **96**, 197001 (2006).
 - [22] C. Panagopoulos, J. L. Tallon, B. D. Rainford, J. R. Cooper, C. A. Scott, and T. Xiang, *Solid State Communications* **126**, 47 (2003).
 - [23] C. Stock, W. J. L. Buyers, Z. Yamani, C. L. Broholm, J.-H. Chung, Z. Tun, R. Liang, D. Bonn, W. N. Hardy, and R. J. Birgeneau, *Phys. Rev. B* **73**, 100504 (2006).
 - [24] J. E. Sonier, F. D. Callaghan, Y. Ando, R. F. Kiefl, J. H. Brewer, C. V. Kaiser, V. Pacradouni, S. A. Sabok-Sayr, X. F. Sun, S. Komiya, et al., *Phys. Rev. B* **76**, 064522 (2007).
 - [25] A. Damascelli, Z. Hussain, and Z.-X. Shen, *Rev. Mod. Phys.* **75**, 473 (2003).
 - [26] A. Kanigel, U. Chatterjee, M. Randeria, M. R. Norman, S. Souma, M. Shi, Z. Z. Li, H. Raffy, and J. C. Campuzano, *Phys. Rev. Lett.* **99**, 157001 (2007).
 - [27] U. Chatterjee, M. Shi, D. Ai, J. Zhao, A. Kanigel, S. Rosenkranz, H. Raffy, Z. Z. Li, K. Kadowaki, D. G. Hinks, et al., *Nature Physics* **6**, 99 (2010).
 - [28] H.-B. Yang, J. D. Rameau, Z.-H. Pan, G. D. Gu, P. D. Johnson, H. Claus, D. G. Hinks, and T. E. Kidd, *Phys. Rev. Lett.* **107**, 047003 (2011).
 - [29] J. Chang, Y. Sassa, S. Guerrero, M. Månsson, M. Shi, S. Pailhès, A. Bendounan, R. Mottl, T. Claesson, O. Tjernberg, et al., *New J. Phys.* **10**, 103016 (2008).
 - [30] R.-H. He, X. J. Zhou, M. Hashimoto, T. Yoshida, K. Tanaka, S.-K. Mo, T. Sasagawa, N. Mannella, W. Meevasana, H. Yao, et al., *New J. of Phys.* **13**, 013031 (2011).
 - [31] M. Hashimoto, R.-H. He, K. Tanaka, J.-P. Testaud, W. Meevasana, R. G. Moore, D. Lu, H. Yao, Y. Yoshida, H. Eisaki, et al., *Nature Physics* **6**, 414 (2010).
 - [32] E. Razzoli, G. Drachucki, A. Keren, M. Radovic, N. C. Plumb, J. Chang, J. Mesot, and M. Shi, preprint (2012).
 - [33] M. R. Norman, A. Kanigel, M. Randeria, U. Chatterjee, and J. C. Campuzano, *Phys. Rev. B* **76**, 174501 (2007).
 - [34] T. Eckl, D. J. Scalapino, E. Arrigoni, and W. Hanke, *Phys. Rev. B* **66**, 140510 (2002).
 - [35] M. Mayr, G. Alvarez, C. Şen, and E. Dagotto, *Phys. Rev. Lett.* **94**, 217001 (2005).
 - [36] D. Valdez-Balderas and D. Stroud, *Phys. Rev. B* **74**, 174506 (2006).
 - [37] Y.-W. Zhong, T. Li, and Q. Han, *Phys. Rev. B* **84**, 024522 (2011).
 - [38] S. Banerjee, T. V. Ramakrishnan, and C. Dasgupta, *Phys. Rev. B* **84**, 144525 (2011).
 - [39] G. Alvarez, M. Mayr, A. Moreo, and E. Dagotto, *Phys. Rev. B* **71**, 014514 (2005).
 - [40] G. Alvarez and E. Dagotto, *Phys. Rev. Lett.* **101**, 177001 (2008).
 - [41] M. Vojta, T. Vojta, and R. K. Kaul, *Phys. Rev. Lett.* **97**, 097001 (2006).
 - [42] M. I. Salkola, V. J. Emery, and S. A. Kivelson, *Phys. Rev. Lett.* **77**, 155 (1996).
 - [43] M. Granath, V. Oganesyan, D. Orgad, and S. A. Kivelson, *Phys. Rev. B* **65**, 184501 (2002).
 - [44] M. Granath and B. M. Andersen, *Phys. Rev. B* **81**, 024501 (2010).